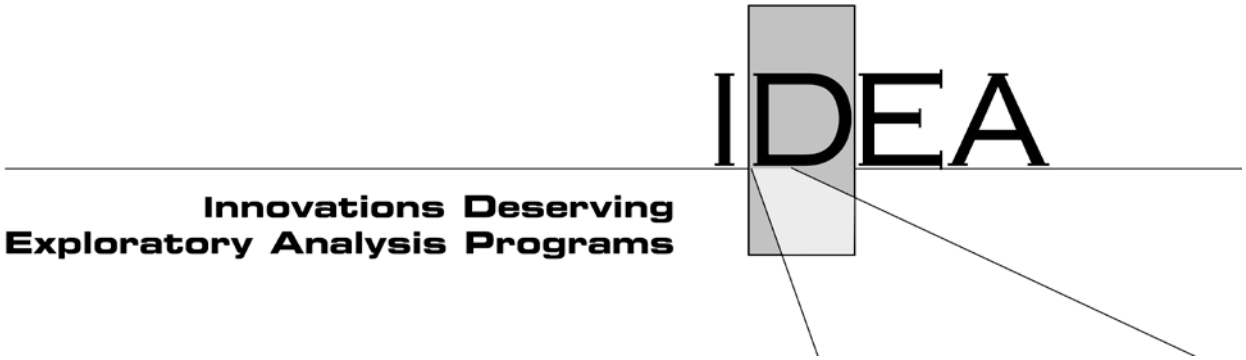

Rail Safety IDEA Program

Remote Sensing with Mobile LiDAR and Imaging Sensors for Railroad Bridge Inspections

Final Report for
Rail Safety IDEA Project 26

Prepared by:
Luis Daniel Otero, Adrian Peter,
Mark Moyou

Florida Institute of Technology

August 2016

TRB TRANSPORTATION RESEARCH BOARD
The National Academies of
SCIENCES · ENGINEERING · MEDICINE

Innovations Deserving Exploratory Analysis (IDEA) Programs Managed by the Transportation Research Board

This IDEA project was funded by the Rail Safety IDEA Program. The TRB currently manages the following three IDEA programs:

- The NCHRP IDEA Program, which focuses on advances in the design, construction, and maintenance of highway systems, is funded by American Association of State Highway and Transportation Officials (AASHTO) as part of the National Cooperative Highway Research Program (NCHRP).
- The Rail Safety IDEA Program currently focuses on innovative approaches for improving railroad safety or performance. The program is currently funded by the Federal Railroad Administration (FRA). The program was previously jointly funded by the Federal Motor Carrier Safety Administration (FMCSA) and the FRA.
- The Transit IDEA Program, which supports development and testing of innovative concepts and methods for advancing transit practice, is funded by the Federal Transit Administration (FTA) as part of the Transit Cooperative Research Program (TCRP).

Management of the three IDEA programs is coordinated to promote the development and testing of innovative concepts, methods, and technologies.

For information on the IDEA programs, check the IDEA website (www.trb.org/idea). For questions, contact the IDEA programs office by telephone at (202) 334-3310.

IDEA Programs Transportation Research Board 500 Fifth Street, NW Washington, DC 20001

Remote Sensing with Mobile LiDAR and Imaging Sensors for Railroad Bridge Inspections

Rail Safety IDEA Program Final Report
Contract Number: Safety-26
Period: August 2014 – August 2016

Prepared for:
Rail Safety IDEA Program
Transportation Research Board
National Research Council

Prepared by:
Luis Daniel Otero, Ph.D., Adrian Peter, Ph.D., and Mark Moyou

Florida Institute of Technology, Dept. of Engineering Systems
150 West University Blvd.
Melbourne, FL 32901

Email: lotero@fit.edu
Phone: (321) 674-7173

ACKNOWLEDGMENTS

This research effort was supported by the National Academies of Sciences, Engineering, and Medicine (NASEM) Transportation Research Board (TRB) Safety IDEA Program. This program is funded by the Federal Railroad Administration.

This research significantly benefited from industry support and guidance provided by CSX and Florida DOT's District 5 personnel, as well as guidance from TRB Project Managers Charles Taylor and Jo Allen Gause. Special thanks to Mr. Ross White, who provided invaluable help and guidance throughout the project, especially during field tests.

In addition, the following Florida Institute of Technology individuals contributed in one way or another to the development of this major research effort: Mr. Frank Kinney, Dr. Muzaffar Shaikh, and Ms. Arlene Grant.

The main author would like to sincerely thank the guidance and support provided by the members of the project's Expert Review Panel:

- Geoffrey Sasser (Bridge Inspector, CSX) – Railroad/Bridge Engineer Expert
- Jerry Bogan, P.E. (Senior Engineer, AECOM) – Railroad/Bridge Engineer Expert
- Nicholas Shorter, Ph.D. (Research Scientist, Lockheed Martin) – LiDAR and Image Processing Expert
- Tarek Omar, Ph.D. (FRA Office of R & D) – Safety IDEA Committee Liaison

The main author would also like to sincerely thank the following faculty and graduate students that formed part of the research team:

- Adrian Peter, Ph.D. (Co-PI, Associate Professor of Engineering Systems)
- Paul Cosentino, Ph.D., P.E. (Co-PI, Professor of Civil Engineering)
- Carlos Otero, Ph.D. (Associate Professor of Electrical and Computer Engineering)
- Mark Moyou (Graduate Student – Systems Engineering)
- Dennis Dalli (Graduate Student – Systems Engineering; UAS Flight Instructor – College of Aeronautics)
- Nick Gagliardo (Graduate Student – Civil and Systems Engineering)
- Javier Merino (Undergraduate Student – Computer Engineering)

The research completed through this funded project would have not being possible without key contributions from the individuals and industry partners mentioned above. Thank you so much for your support!!

TABLE OF CONTENTS

TABLE OF FIGURES

TABLE OF TABLES

1 EXECUTIVE SUMMARY

This report describes results from a research effort to investigate the applicability of two remote sensing approaches –one based on Light Detection and Ranging (LiDAR) and the other one on imaging sensors—to help detect concrete cracks and displacement of bridge components. This overall objective was decomposed into three research objectives. The first research objective included developing and evaluating prototype image processing algorithms for concrete crack detection and classification. The second research objective included developing and evaluating three-dimensional (3D) models from LiDAR data to identify signs of bridge component displacements. The third research objective included evaluating the effects to the image processing algorithms and 3D models with data collected using an unmanned aerial system (UAS). The solution approach to address these three research objectives was divided into two project stages. The first two research objectives corresponded to project stage 1, and the third research objective corresponded to project stage 2. Research questions corresponding to both project stages and their related research objectives were developed to guide the overall research study.

Prototype image processing algorithms were developed to detect and classify concrete cracks. For the detection problem, a five-step algorithm based on an unsupervised learning approach was developed in Matlab to extract pixels that belong to concrete cracks from images. For the classification problem, the objective was to process the resulting binary images from the detection algorithm to identify cracks as transversal, longitudinal, block, or alligator. The algorithms were tested with images collected from field tests. The images included different types of concrete cracks, along with various types of noise factors. The algorithms were successful in detecting and classifying different types of concrete cracks from various images. Contrary to previous studies found in the academic literature, these images were collected from field tests and used as inputs to the detection algorithm without any preprocessing activity.

Various tests were conducted to gain insights into the applicability of 3D models developed from mobile LiDAR data to identify signs of bridge settlement and displacement of bridge columns. The mobile LiDAR sensor used for data collection was a Velodyne HDL-32E. The first set of tests involved LiDAR data acquisition using a controlled sensor location approach. For these tests, a customized tripod mount was developed to control the sensor's position, thus facilitating the alignment of LiDAR data into a locally defined coordinate system to develop 3D models. The general solution approach involved test planning, collecting data, aligning LiDAR data into a common coordinate system, developing 3D models, and evaluating the use of the resulting models to identify structural deviations. A mockup bridge structure was developed using PVC material to conduct initial experiments prior to conducting more expensive field tests. Prior to data collection, the LiDAR sensor was placed on the tripod mount at a distance of *x* feet from the PVC structure, and a portion of the PVC structure was inclined *y* inches using 0.5 inch thick wooden stakes. The resulting 3D models showed that 0.5 inch inclinations were easily identified with the sensor located 10 feet from the structure, and using only 20 LiDAR scans. It can be safely assumed that more scans at different sensor locations would result in denser 3D models, which would improve the usability of the 3D models for detecting vertical and horizontal displacement of bridge components. Overall, results highlighted the potential value of 3D models for bridge inspection purposes using controlled sensor locations.

The next step of the research effort was to evaluate the applicability of 3D models developed from LiDAR data collected using a UAS instead. To achieve this objective, a customized UAS with integrated LiDAR sensor and other subsystems was developed for effective LiDAR data acquisition of bridge structures. Indoor and outdoor UAS tests were conducted to collect LiDAR data of bridge structures for developing 3D models. Comparisons between the resulting 3D models from the UAS data acquisition approach versus those from the controlled sensor location approach indicated that there was no noticeable difference between them. It was concluded that a UAS approach is highly capable of resulting in 3D models of high practical value during bridge inspections.

Results from this initial research effort positively highlighted the potential practical value from using UAS and sensor technology for bridge inspection purposes. Industry support from CSX and Florida Department of Transportation (DOT) throughout this research effort was essential to fully address the research questions that guided this study. The overall consensus from industry partners was that this technology has the potential to mature into a bridge inspection system that could positively and significantly impact performance, effectiveness, and safety associated with bridge inspections. Some future research directions that were identified to realize such a system include: automatic detection of concrete and steel

cracks using a deep learning approach; development of crack maps for bridge structures; capability for autonomous UAS flights to collect bridge sensor data; software development to integrate data from various sensor types; and extensive outside UAS field tests for full evaluation.

2 INTRODUCTION AND PROBLEM STATEMENT

Railroad bridges are critical components of transportation infrastructures. In the United States, there are more than 76,000 railroad bridges that cover over 1,700 miles [*1*]. Many bridge spans currently in service are approaching 100 years of age [*2*]. To ensure safe operations within the railroad system, maintenance and routine railroad bridge inspection activities are critical. Routine visual inspections are used to develop structural health ratings of bridges, which serve as a measure of their structural quality. Any sign of structural distress (e.g., concrete cracks) found during inspections can significantly impact the structural health rating of a bridge. Once evidence of a structural distress is identified, resources can be properly allocated to find the distress cause(s) and move towards corrective actions.

From a systems engineering perspective, the quality of onsite visual inspections of bridges can be defined in terms of various quality attributes. For example, overall inspection cost can be defined as a quality attribute that is affected by the number of man-hours spent by an inspection crew, the cost incurred in renting inspection equipment, and any cost associated with delaying train passage during inspections, among others. Other quality attributes to be considered are safety of inspectors during inspections, the effectiveness of the inspection team to detect/classify structural defects (i.e., distress signs), and accessibility to hard-to-reach structural elements during inspections (e.g., top chord of a truss drawbridge). The current on-site visual bridge inspection process of railroad bridges is an effective approach to identify/classify structural defects. However, the overall quality of this process is affected because it is relatively expensive, is time consuming, often puts inspectors in high risk situations, and may cause train delays. These limitations highlight the need to follow a continuous improvement mentality by developing novel approaches to help improve the overall quality of onsite bridge inspections.

Remote sensing approaches to collect data from bridge components for analysis and evaluation can potentially improve the overall quality of bridge inspections. If proven effective, remote sensing methods for bridge inspections may positively impact overall inspection costs, inspectors' safety, train delays during inspections, and access to data from hard-to-reach structural components for defect evaluations. Therefore, it is necessary to conduct research studies to investigate the capability of remote sensing approaches to help detect and classify structural distress signs during bridge inspections.

2.1 RESEARCH OBJECTIVES AND RESEARCH QUESTIONS

There are various types of structural distress signs that can be identified during bridge inspections. These signs may reflect structural defects that affect—or will potentially affect—the capability of a bridge to support the load that it was designed for. One of the most common critical signs of structural distress is concrete cracking [*1*]. Concrete cracking can lead to corrosion of inner reinforcing steel bars; thus gradually reducing the strength of the structure and affecting its lifespan. In addition, concrete cracks are often evidence of initial fatigue reactions of bridge components [*2, 3*].

Another critical sign of structural distress is displacement of bridge components. For example, bridge settlement (i.e., vertical displacement of a bridge) can result in the formation of cracks within the deck, superstructure, or substructure [*4*]. Figure 2-1a provides an image that shows a bridge settlement displacement of around 5 to 8 centimeters [*5*]. Another example is displacement of bridge piles, which can result in significant additional stress to other critical members. For example, Figure 2-1b shows battered/angled piles supporting a bridge's deck. Additional deviations to these piles could increase the probability of overall bridge failure.

The overall goal of this research study is to investigate the applicability of two remote sensing approaches to help detect concrete cracks and displacement of bridge components. For one of the approaches, data were collected using imaging sensors, whereas the other approach employed a mobile Light Detection and Ranging (LiDAR) sensor. The remote sensing capabilities of LiDAR sensors, coupled with the proper knowledge to develop high-quality three-dimensional

(3D) models from collected LiDAR data, could make this type of sensor technology a valuable tool during transportation infrastructure inspections. Table 2-1 presents the three main research objectives (Res_Obj) that were identified to address the overall goal of this research study.

The solution approach to achieve the research objectives was divided into two project stages. Stage 1 involved planning activities, development of prototype image processing algorithms to detect and classify concrete cracks, and development of 3D bridge/structure models from LiDAR sensor data to detect displacement of bridge components. Stage 2 involved

Figure 2-1 Examples of (a) bridge settlement and (b) battered piles.

evaluating the applicability of the image processing algorithms with image data collected using an unmanned aerial system (UAS). This stage also involved the development of a customized UAS with integrated mobile LiDAR sensor for bridge inspection purposes. The custom-built UAS was used to collect LiDAR data of a scaled-down bridge structure during indoor experiments and of a real railroad bridge during outdoor field tests. The collected data were used to develop 3D models of the bridge structures to draw conclusions regarding the applicability of such models for bridge inspection purposes. Tables 2-2 and 2-3 show the research questions corresponding to both project stages and their related research objectives. These questions guided this research study.

Table 2-1 Research objectives to achieve the overall research goal

No.	Research Objective
Res_Obj #1	Develop prototype image processing algorithms for detection and classification of concrete cracks, considering aspects that significantly affect the practical value of current approaches
Res_Obj #2	Evaluate the applicability of 3D models developed from LiDAR sensor data collected at fixed locations to identify signs of bridge component displacement
Res_Obj #3	Evaluate Res_Obj #1 and #2 using data collected from imaging and LiDAR sensors integrated into an unmanned aerial system (UAS)

Table 2-2 Research questions for Stage 1

No.	Research Question
1.1	What factors significantly affect the practical value of current image processing algorithms for concrete crack detection and classification? (*Res_Obj #1*)
1.2	How can a concrete crack detection algorithm that considers aspects that significantly affect the practical value of current approaches be developed? (*Res_Obj #1*)
1.3	How can a concrete crack classification algorithm that considers aspects that significantly affect the practical value of current approaches be developed? (*Res_Obj #1*)
1.4	What is the applicability of 3D models developed from mobile LiDAR data—collected at fixed locations—to help identify signs of bridge settlement and displacement of bridge piles? (*Res_Obj #2*)

Table 2-3 Research questions for Stage 2

No.	Research Question
2.1	How effective are the detection and classification prototype image processing algorithms from Stage 1 when image data are collected using a UAS? (*Res_Obj #3*)
2.2	How is the applicability of 3D models developed from LiDAR data impacted if data were collected using a UAS? (*Res_Obj #3*)

2.2 Scope and Organization of Report

This report is organized into six sections. Section 3 describes research studies related to image processing techniques for detection and classification of concrete cracks, as well as studies that developed 3D models from LiDAR data for transportation infrastructure applications. Section 4 describes the prototype image processing algorithms developed to detect and classify concrete cracks. Section 5 presents experiments conducted to develop 3D models of bridge structures from LiDAR data, and an evaluation of the applicability of these models to detect bridge settlements and deviations. Section 6 presents concluding remarks and recommendations for future research efforts.

3 REVIEW OF RELEVANT LITERATURE

The following subsections present a description of research studies related to image processing techniques for concrete crack detection and classification, as well as studies that developed 3D models using LiDAR data for transportation infrastructure applications. The literature review effort also includes studies related to using UAS during structural inspections. Each subsection concludes with a summary of key findings.

3.1 Studies on Image Processing for Concrete Crack Detection and Classification

Table 3-1 presents a list of relevant studies related to the application of image processing techniques for detecting and classifying concrete cracks. This table shows that in recent years, multiple algorithms for automated concrete crack detection have been proposed. However, the effectiveness of these algorithms have been significantly affected by variations in surface textures and image quality, which are highly dependent on environmental and lighting conditions [*6*]. Image variability created by non-uniform illumination, shadings on bridge surfaces, and the presence of particular artifacts (e.g., oil, stains, and bridge fixtures) makes it very difficult for algorithms to automatically distinguish concrete cracks from their backgrounds [*3*, *6*]. These limitations significantly affect the practical value of such algorithms for real-life applications. Therefore, there is a need for developing further research studies to advance the state of the art in the area of image processing algorithms for detection and classification of concrete cracks.

3.1.1 *Specific Methods for Crack Detection and Classification*

The literature review effort also resulted in the identification of four specific methods for crack detection and classification. These methods are histogram-based techniques, mathematical morphological tools, learning techniques, and filtering. Histogram-based techniques are the most popular methods for detection and classification. These approaches convert the histogram of an image into a probability distribution. That is, these methods assume that the two gray level distributions (i.e., concrete surface and crack) can be separated based on global level statistics such as mean and standard deviation. Based on this assumption, histograms extracted from images can be used to segment the images. Segmentation is the process of grouping similar parts of an image together, where similarity is based on some measure such as a grayscale intensity threshold. Examples of this technique can be found in [*7–11*]. These approaches are simple and not time consuming, but may result in a significant number of false detections [*3, 12*]. Another issue with the threshold method is that it does not ensure proper connectivity of concrete crack alignments [*2*]. To effectively use histogram-based techniques, pixels belonging to a crack in an image must be darker than the image's background (i.e., surface). Another requirement is that the gray level distribution of a crack and the background are independent, allowing for a single threshold to be applied.

Table 3-1 Relevant work using image processing for crack detection and classification

Title	Application	Reference
Automatic Bridge Crack Detection—A Texture Analysis-Based Approach	Crack Detection	[*13*]
Image-Based Retrieval of Concrete Crack Properties for Bridge Inspection	Crack Detection	[*14*]
Crack Image Processing Using Probability—Based Threshold	Crack Detection	[*15*]
Intelligent Crack Detecting Algorithm on Concrete Crack Images Using Neural Networks	Crack Detection and Classification	[*16*]
An Efficient Crack Detection Method Using Percolation-Based Image Processing	Crack Detection	[*17*]
Crack Detection in Concrete Surfaces Using Image Processing, Fuzzy Logic, and Neural Networks	Crack Detection	[*18*]
Automated Image Processing Technique for Detecting and Analyzing Concrete Surface Cracks	Crack Detection and Classification	[*2*]
Automatic Road Crack Detection and Characterization	Crack Detection and Classification	[*11*]

3.1.2 *Specific Methods for Crack Detection and Classification*

The literature review effort also resulted in the identification of four specific methods for crack detection and classification. These methods are histogram-based techniques, mathematical morphological tools, learning techniques, and filtering. Histogram-based techniques are the most popular methods for detection and classification. These approaches convert the histogram of an image into a probability distribution. That is, these methods assume that the two gray level distributions (i.e., concrete surface and crack) can be separated based on global level statistics such as mean and standard deviation. Based on this assumption, histograms extracted from images can be used to segment the images. Segmentation is the process of grouping similar parts of an image together, where similarity is based on some measure such as a grayscale intensity threshold. Examples of this technique can be found in [*7–11*]. These approaches are simple and not time consuming, but may result in a significant number of false detections [*3, 12*]. Another issue with the threshold method is that it does not ensure proper connectivity of concrete crack alignments [*2*]. To effectively use histogram-based techniques, pixels belonging to a crack in an image must be darker than the image's background (i.e., surface). Another requirement is that the gray level distribution of a crack and the background are independent, allowing for a single threshold to be applied.

Mathematical morphological operations are used to process both binary and grayscale images based on shapes. These techniques are based on a thresholding method, which basically means applying a threshold to a grayscale image. In [*19*], the authors proposed a crack detection system composed of four main stages: black pixel extraction, saddle point

extraction, linear feature extraction, and connection processing. Although these methods require an initial thresholding, the results contain fewer false detections than methods based on histogram analysis [*3*].

There are four basic morphological operations: dilation, erosion, opening, and closing. These operations take binary or grayscale images as input along with a structuring element, and return a processed image as an output. The structuring element can be thought of as a user-defined object that is used to gather specific pixels from the image on which to perform the four operations on the image. The size and shape of the structuring element determines which group of pixels the operations will be applied to [*20*]. The quality of the results is highly dependent on the size and type of structuring element. A key requirement that must be met to effectively use mathematical morphological techniques is that crack pixels must be darker than surface/background pixels. Another key requirement that must be met is that concrete cracks are shown as continuous thin objects in an image.

Learning techniques, which are often based on neural networks (NN), were developed to overcome some of the issues related to histogram-based and mathematical morphological methods. The two main types of learning approaches are supervised and unsupervised learning. The supervised approach requires training data to build a model for detection and classification purposes. For example, a concrete crack detection algorithm would be fed a large number of images of different types of concrete cracks. The NN algorithm will use features (e.g., edges, intensity) extracted from the images to estimate a model. The model can then be used to process other images to detect whether or not they contain concrete cracks. A similar approach can be followed for a crack classification model after successfully detecting a concrete crack in an image.

Unsupervised learning does not require data. Features are also extracted in this approach, but the images are labeled based on similar objects. For instance, if useful features are chosen, images that contain concrete cracks would be grouped together. Similarly, images without cracks would be grouped separately. For example, during image classification of concrete cracks, it could be expected that images with longitudinal cracks be grouped together, images with transversal cracks be grouped together, and so on. Examples of these approaches can be found in [*6, 11, 21]*.

The filtering technique is mainly based on the assumption that cracks do not have constant widths. Some of the most popular filtering techniques use edge extraction, wavelet detections [*22–24*], contourlets detection [*25*], Gabor filters, finite impulse response filter, and methods based on partial differential equations. In [*22*], the authors perform a comparison of the effectiveness of the following four edge detection techniques that could be used for crack detection in concrete bridges: Fast Haar transform (FHT), Fast Fourier transform (FFT), Sobel, and Canny. These algorithms were implemented in Matlab and simulated using a sample of 50 concrete bridge images (25 of the images included concrete cracks and 25 did not). The results showed that the FHT technique was significantly more reliable than the other three. In this study, the threshold was defined as the average value of the intensity of all pixels in the crack images. In [*12*], the authors presented a methodology for adapting a multi-resolution-based segmentation. First, the edges are thresholded at different scales, and the resulting binary images are combined in a reconstructed gradient-like image. Then, the watershed algorithm is applied. This method is quantitatively validated on reference segmentations and compared to an adapted filtering and Markovian modeling algorithm.

3.1.3 SUMMARY OF KEY FINDINGS

Following is a list of key findings that resulted from the literature review effort on image processing techniques for concrete crack detection and classification:

- Most studies focus on the problem of detecting and classifying concrete cracks using as input images that only contain cracks (i.e., without any other background objects such as trees or other bridge components).
    - These studies assume that a reliable crack detection algorithm is already in place to provide input images to their crack classification algorithms.
- One of the most popular techniques involves splitting the image into blocks and performing detection and classification on these individual blocks. The results are then used to make a consensus about the entire image. However, the technique of processing an image as a whole to detect and classify cracks has not been fully addressed.

- There is no completely automatic system that performs crack detection and classification on images that contain both crack and non-crack objects (such as pipes, debris, trees, people). The problem of detecting cracks in the presence of these other objects is a significant problem that has not been addressed sufficiently.
- Cracks are considered as local defects on images since a crack can even represent less than 1.5% of the whole image [*26*].
- One of the main drawbacks of most methods proposed in the literature is that the detection results contain a significant number of false detections and false negatives if applied to images with different backgrounds (i.e., the performance of the method is highly dependent on the surface texture).
- Although the literature makes it clear that the quality of the results from detection algorithms is strongly related to the quality of the image acquisition process, most studies fail to explain their image acquisition process. In fact, there are studies that do not provide any details about the images used in their proposed detection and classification algorithms.
- Most of the studies found in the literature highlight the importance of preprocessing images due to the noise and non-uniform illumination effects present on the images [*3, 6, 11*]. However, very few details regarding the hardware (e.g., camera, lighting bulbs, laser, and others) and illumination conditions (e.g., natural light or controlled light) are provided.
- Images will need to be preprocessed no matter if they were acquired under natural or controlled light conditions. Nevertheless, images obtained without controlled light require more pre-processing time and robust techniques to reduce shadow and illumination effects. The lighting system must be designed in such way to preserve the crack signal, which sometimes is not well contrasted with concrete surfaces.
- Concrete crack detection and classification systems have been the center of research studies for almost three decades. Although several of these proposed studies show promising results, a general solution that provides reliable results on a continuous basis is currently non-existent.
- The literature lacks a standard benchmarking protocol for evaluating and comparing different concrete crack detection and classification methods.
- The development of a full-blown automated crack detection and classification system continues to be a topic of high interest to researchers due to complex challenges that need to be overcome.

3.2 LiDAR Sensor and UAS for Transportation Infrastructure Applications

UAS equipped with mobile LiDAR sensors may be useful tools during bridge inspections. However, there is a lack of studies in the academic literature related to the use of such aerial platforms with integrated mobile LiDAR sensors for bridge inspections. Table 3-2 presents a list of relevant studies in the area of LiDAR and/or UAS for bridge inspections.

Table 3-2 Relevant work with LiDAR and/or UAS for monitoring/inspecting transportation structures

Title	Application	Reference
Light Detection and Ranging (LiDAR) Technology Evaluation	Infrastructure Inspections	[27]
Infrastructure Investment Protection with LiDAR	Infrastructure Inspections	[28]
Pilot Study on Laser Scanning Technology for Transportation Projects	Infrastructure Inspections	[29]
LiDAR 3D High Density Scanning (HDS) Bridge Scan	Bridge Inspections	[30]
LiDAR for Data Efficiency	Highway Inspections	[31]
LiDAR-Based Bridge Structure Defect Detection	Bridge Inspection	[32]
Develop a UAV Platform for Automated Bridge Inspection	Bridge Inspections	[33]
CALTRANS Bridge Inspection Aerial Robot	Bridge Inspections	[34]
Evaluation and Development of Unmanned Aircrafts for UDOT Needs	Monitoring Infrastructures	[35]
Proof of Concept for Using UAVs for HML and Bridge Inspections	Bridge Inspections	[36]

3.2.1 SUMMARY OF KEY FINDINGS

Following is a list of key findings that resulted from the literature review effort on the use of LiDAR systems and/or UAS for structural inspections:

- Studies that involve both UAVs and LiDAR systems for the specific purpose of bridge inspections are very scarce, and for inspection of railroad bridges are nonexistent. This lack of studies presents an opportunity to investigate the use of a LiDAR-UAS system for railroad bridge inspections.
- The literature highlights the potential for using LiDAR for structural inspections due to the ability of data collection during day and night, minimization of personnel safety issues, minimization of data collection time, and potential reduction of costs.
- Some studies assume that the accuracy of mobile scanning systems may be less than the one of fixed scanners. However, it is also mentioned that the high mobility, capture of multiple areas, fusion of multiple sensors, and huge amounts of data collected in short periods of time will combine to enable new approaches to transportation applications.
- Some of the challenges for effective implementation of LiDAR technology include inspectors' lack of experience with remote sensing techniques, data management challenges due to enormous amounts of data, and software limitations.
- The literature shows a consensus regarding the belief that structural measurements and displacements can be extracted from LiDAR point clouds.
- The literature provides evidence on the potential significant benefits that can be realized with the use of UAS for bridge inspections.

4 DEVELOPMENT AND EVALUATION OF CONCRETE CRACK DETECTION AND CLASSIFICATION ALGORITHMS

This section describes the research approach taken to develop image processing algorithms for concrete crack detection and classification, considering aspects that significantly affect the practical value of current approaches.

4.1 DEVELOPMENT OF CONCRETE CRACK DETECTION ALGORITHM

The process of identifying individual objects in digital images and videos is known as object detection. The two classes of algorithms used in object detection are supervised and unsupervised learning algorithms. Unsupervised algorithms discover structure in the data and do not require training data. However, these types of algorithms do not perform well unless the features used (e.g., edges, gradients, intensity) are reliable. Supervised algorithms, on the other hand, require training with image data containing various classes of objects required to be identified (e.g., various types of concrete cracks).

Figure 4-1 shows an example of a concrete crack on a bridge. Most people can easily identify the concrete crack in the figure because they can immediately detect the various colors and patterns that make up the image. For an algorithm, however, the task of detecting the crack within the image is different because the image is represented as a matrix of numbers called "pixel intensity values." This numerical representation is called "digitizing" the image. Therefore, the crack detection task becomes an issue of obtaining optimal pixel intensity values, and developing an algorithm capable of processing these intensity values to effectively detect the concrete crack in the image.

Figure 4-1 Example of a concrete crack on a bridge.

The concrete crack detection algorithm developed for this research study is congruent with the protocol that is present in the current literature—that of extracting the pixels that belong to cracks from images that already contain cracks. An unsupervised learning approach was developed for the concrete crack detection problem, thus avoiding the need to gather a large number of training images that are typically required for training supervised learning algorithms. The entire algorithm was implemented in Matlab. The purpose of the detection algorithm was to extract pixels that belong to concrete cracks from images. The steps of the crack detection algorithm are:

- Step 1: Grayscale Image Closing
- Step 2: Anisotropic Diffusion
- Step 3: Sobel Edge Detection
- Step 4: Active Contours
- Step 5: Morphological Noise Removal

The output from these steps is a binary image that is used to perform crack classification.

4.1.1 STEP 1: GRAYSCALE IMAGE CLOSING

Image closing is an image processing technique belonging to the family of morphological operations. Typically, these operations are applied to binary images (i.e., black and white); however, the grayscale equivalent can be used. Applying these operations requires a structuring element, which can be thought of as a stencil that is slid across an image for certain effects to take place. The resulting effects depend on the operation being performed, as well as the size and type of the structuring element. Image closing preserves background regions that have a shape similar to that of the structuring element used, or that can completely contain the structuring element itself. Other regions that do not fit these criteria are excluded from further processing. A comprehensive description regarding the effects of image closing is presented in [*37*].

The algorithm developed for the crack detection problem uses line-shaped structuring elements. That is, the algorithm will attempt to exclude regions that are not line-shaped from an image. This process is often not easily seen in grayscale. A total of five separate line structuring elements of size 3 pixels oriented at 0, 90, 45, 60, and -45 degrees were used. The effect of this grayscale closing approach to an original image is shown in Figure 4-2. The closed image in Figure 4-2b seems to be blurred, and the small circular block dots in Figure 4-2a are not as easily visible in Figure 4-2b. This process reduces the noise in the image and allows for much better detection capabilities.

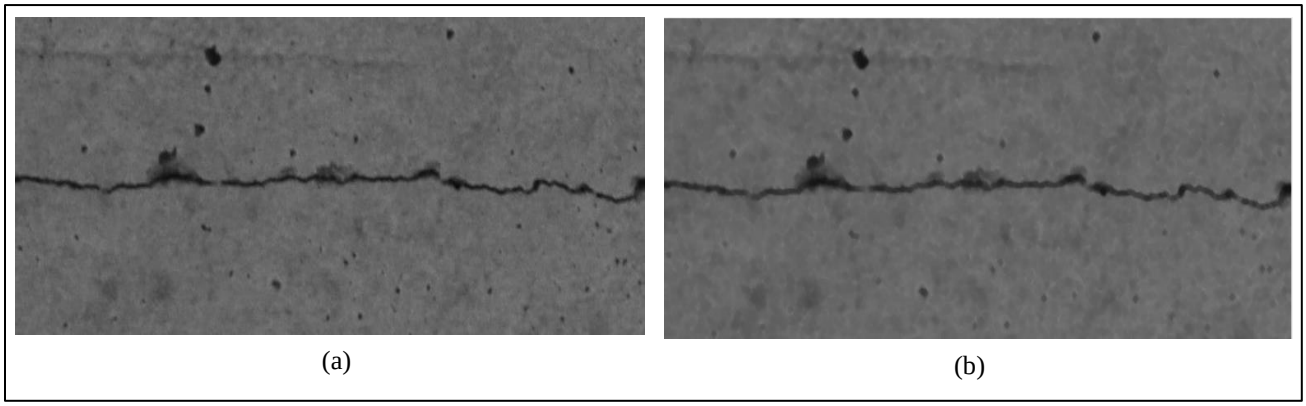

(a) (b)

Figure 4-2 (a) Original image (b) Image showing grayscale image closing.

4.1.2 STEP 2: ANISOTROPIC DIFFUSION

Image blurring is an appropriate technique to smooth out the texture in the background of images that include concrete cracks, resulting in more uniform backgrounds. Contrary to traditional image blurring techniques, anisotropic diffusion preserves edges of concrete cracks or dark regions [*38*]. The effects of the anisotropic diffusion blurring technique on the grayscale closed image from Figure 4-2b is shown in Figure 4-3a. The effects include significant image blurring and preservation of black edges, including non-crack regions. The resulting edge-preserved image will serve as input to an edge detection algorithm.

4.1.3 STEP 3: SOBEL EDGE DETECTION ALGORITHM

The Sobel edge detection algorithm is used to extract edges from images. This algorithm is very efficient when dealing with edges running vertically and horizontally, which are the basic directional components of cracks. Figure 4-3b shows the effect of the edge detection algorithm on the image that was smoothed using anisotropic diffusion (i.e., Figure 4-3a). This figure clearly highlights crack edges, along with some other dark regions which are considered noise; therefore, they will need to be removed at later stages. Furthermore, the output image from the edge detection process provides the boundary of the crack and noise objects. The next step is to extract the internal pixels of the crack inside the edges by using a method called "active contours."

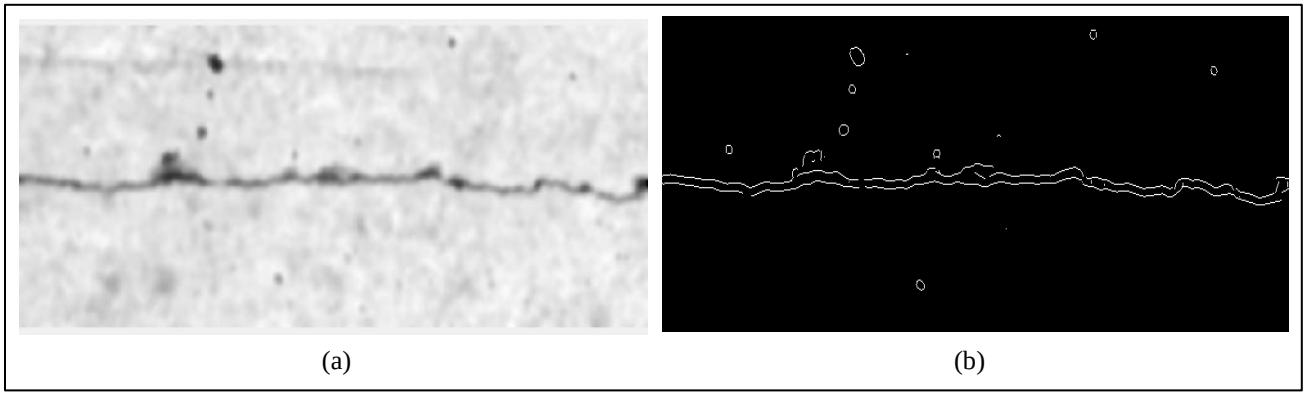

(a) (b)

Figure 4-3 Resulting images from (a) anisotropic diffusion technique and (b) Sobel detection algorithm.

4.1.4 *STEP 4: ACTIVE CONTOURS*

Active contours is a segmentation technique that separates an image into foreground and background regions. This technique works best when it is initialized with the boundaries of objects to be segmented. The algorithm uses the image resulting from the Sobel edge detection algorithm (Figure 4-3b) for initialization and finds the complete contour around objects in the image. These contours are filled to form the image shown in Figure 4-4. Each of the enclosed white regions in the figure is referred to as "blobs." Each of these blobs has morphological properties such as area, orientation, and length. These properties are used to suppress blobs that do not correspond to cracks (i.e., noise blobs).

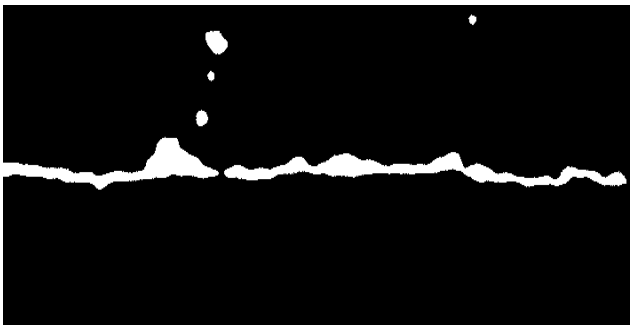

Figure 4-4 Resulting image after segmentation using active contours.

4.1.5 *STEP 5: MORPHOLOGICAL NOISE REMOVAL*

There are two steps for the algorithm to remove noise blobs. First, the areas of all the image blobs are normalized into a 0–1 range by using their area properties. Second, the algorithm identifies noise blobs based on a predefined blob area threshold value of 0.25. That is, any blob with an area less than this threshold is removed from the image. This arbitrary threshold value was set assuming that a blob associated with concrete cracks will have a larger area than the noisy blobs. The resulting image from the detection image processing algorithm is shown in Figure 4-5a. The image shows that using the arbitrary threshold of 0.25, a small part of the crack was removed; however, this will not affect the results from a subsequent crack classification algorithm process. Figure 4-5b shows the crack mask overlaid on the original image.

4.2 DEVELOPMENT OF CONCRETE CRACK CLASSIFICATION ALGORITHM

This section discusses the concrete crack classification process developed to automatically determine crack types from images. First, the resulting binary mask from the crack detection algorithm, shown in Figure 4-5a, was grouped into a 5x5 mask. In this figure, the crack pixels (i.e., white area) have a value of one, and the background pixels (i.e., black area) have a value of zero. Second, a block processing algorithm was employed. If more than 10% of the pixels in the 5x5 block were

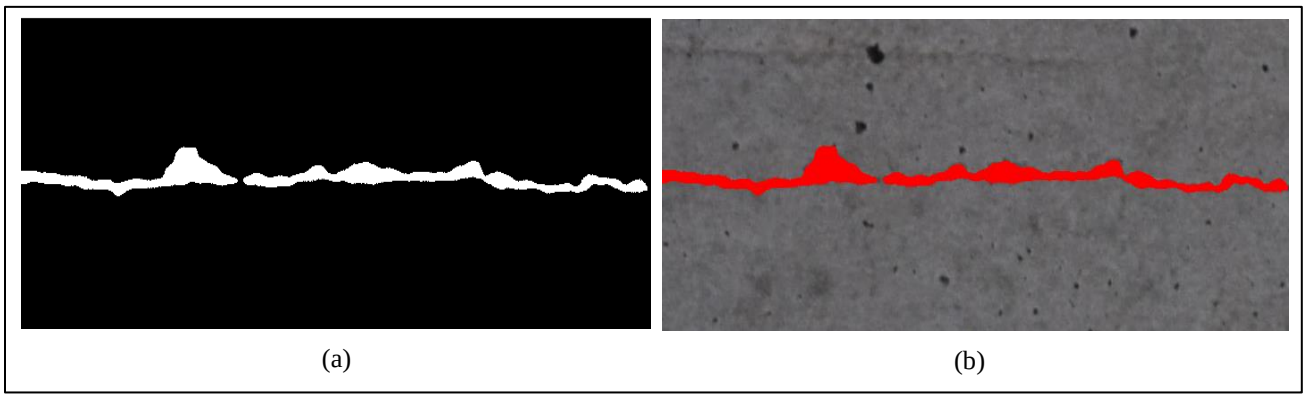

Figure 4-5 (a) Final crack detection mask (b) overlaid on original image.

crack pixels, then the block was labeled as a crack block. This approach removes sharp edges in the crack and prepares the algorithm to perform statistical analysis on the new crack image. Figure 4-6 shows the resulting crack block image.

Figure 4-6 Crack block image from 5x5 block processing.

Using this new crack block image, the algorithm can now obtain vertical and horizontal histograms of the image. The vertical histogram represents the number of crack blocks that exists in each column going down the rows. The number of bins in the vertical histogram is equal to the number of columns in the image matrix. For the horizontal histogram, the number of crack blocks in each row is computed and the number of bins becomes the number of rows. The standard deviation of each of these histograms is then computed. These standard deviations are used as coordinates on a crack classification graph, where *x_stdev_VH* denotes the standard deviation of the vertical histogram, and *y_stdev_HH* denotes the standard deviation of the horizontal histogram. The slope of the line from the point (0,0) to (*x_stdev_VH*, *y_stdev_HH*) determines the type of crack on the image.

The following four common types of concrete cracks were considered: transversal, longitudinal, block, and alligator. Figure 4-7 shows the crack classifications. If the slope of a line is less than 0.4, then the crack is classified as transversal (shown as Region I). If the slope of a line is greater than 2.5, then the crack is classified as a longitudinal (shown as Region II). Any slope that is greater than 0.4 and less than 2.5 results in classifying a concrete crack as either block or alligator (shown in Region III). In order to classify a crack as alligator or block, the percentage of crack blocks in the crack block image relative to the total number of blocks in the image is considered. If the percentage of crack blocks is greater than 20%, then the crack is classified as an alligator crack; otherwise, it is classified as a block crack. The example presented in Figure 4-7 shows a transversal crack because the slope of the line falls in Region I (denoted by the yellow colored diamond).

4.3 CONCRETE CRACK DETECTION AND CLASSIFICATION RESULTS

This section presents results obtained from applying the concrete crack detection and classification algorithms to concrete crack still images collected from bridges during field tests. Figure 4-8 shows an example of a transversal concrete crack. The figure shows (a) the grayscale image, (b) the crack detection mask, and (c) the crack classification graph. Figures 4-9 and 4-10 show examples of longitudinal and block cracks, respectively.

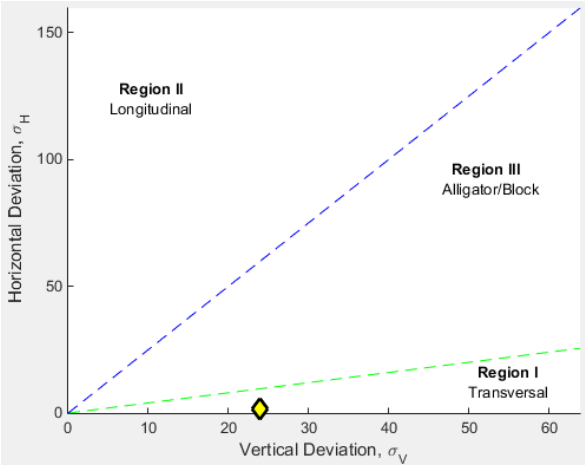

Figure 4-7 Concrete crack classification graph.

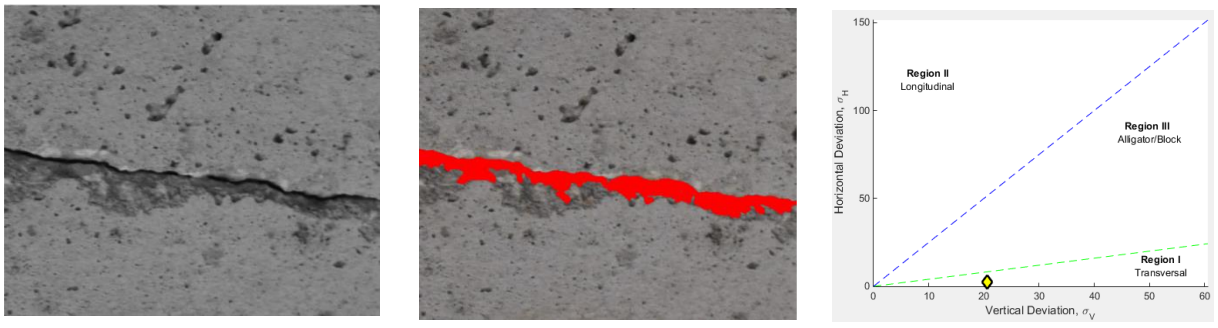

Figure 4-8 Transversal concrete crack (a) grayscale image (b) detection mask (c) classification.

4.4 Evaluation of Concrete Crack Detection and Classification Algorithms Using Data Collected with UAS

Imaging data of different types of concrete cracks on a bridge in Melbourne, Florida, were collected and used to evaluate the image processing capabilities of the algorithms developed in Stage 1 of this project. Using a GoPro camera attached to a small UAS, video footage of concrete cracks on varying concrete surfaces of the bridge was captured. From the video footage, individual video frames were processed to identify concrete crack images. Contrary to studies presented in the literature, the resulting frames do not isolate concrete cracks to facilitate the detection process.

4.4.1 Evaluation of Concrete Crack Detection Algorithm Using Data from UAS

The detection process involves segmenting (i.e., identifying) the pixels that belong to concrete cracks in images. The data collection resulted in 53 concrete crack images that contained diverse concrete surfaces not typically seen in the literature. Figure 4-11a shows a concrete crack image collected from the bridge. Figure 4-11b shows the results from the detection algorithm, which clearly isolates the concrete crack in the image. As shown in the figure, the background (i.e., concrete surface) is very granular and not smooth. These results showed that the detection algorithm developed in Stage 1 is capable of effectively isolating this particular concrete crack in this particular noisy background.

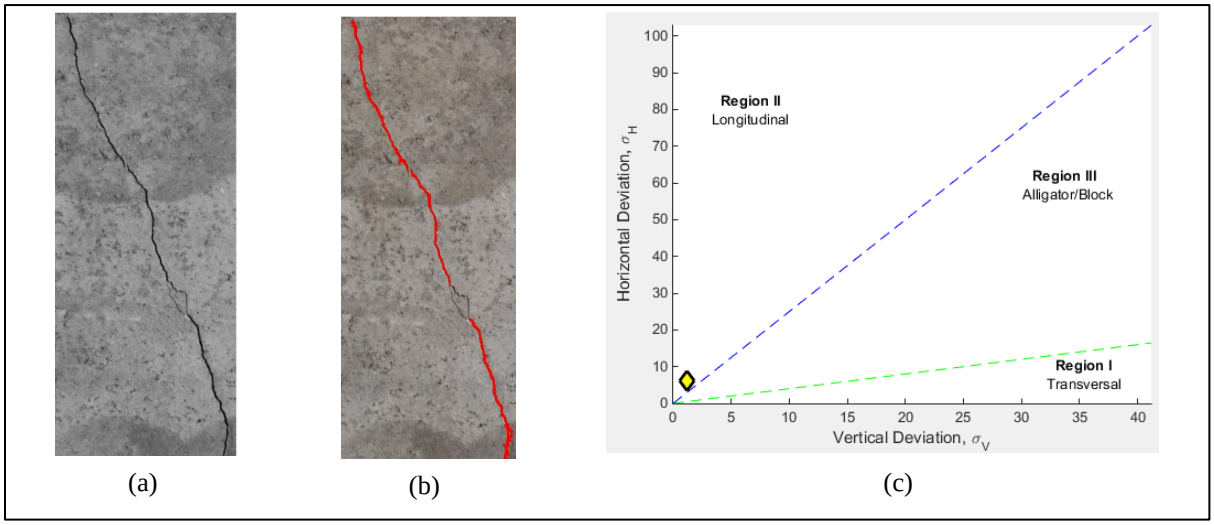

Figure 4-9 Longitudinal crack (a) grayscale image, (b) detection mask, and (c) classification graph.

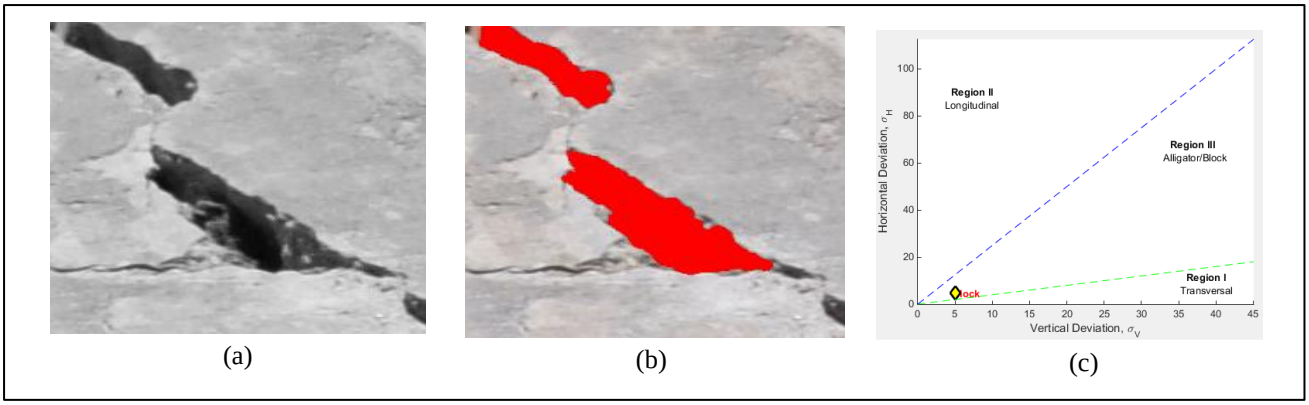

Figure 4-10 Block crack (a) grayscale image, (b) detection mask, and (c) classification graph.

Figure 4-12a shows an example of a very noisy concrete crack image that was collected from the bridge. Here, the background surface is extremely granular, and many regions of the image are similar to the main concrete crack itself. Figure 4-12b shows that the detection algorithm was able to isolate the majority of the crack pixels with some minor errors. Figure 4-13 shows another example of concrete crack detection on granular concrete. These results highlight the potential of the initial prototype detection algorithm.

4.4.2 Evaluation of Concrete Crack Classification Algorithm Using Data from UAS

The classification algorithm from Stage 1 was developed to identify three classes of concrete cracks: longitudinal, transversal, and block. The 53 images collected from the bridge using a UAS in Stage 2 included only transversal and longitudinal concrete cracks; therefore, the classification algorithm was evaluated based on these two types of concrete cracks. Table 4-1 shows a confusion matrix with the resulting classifications for the images processed. The results showed that 83% of the images were accurately classified (i.e., 44 of 53 images). More specifically, of 26 images containing transversal concrete cracks, 20 were accurately classified as transversal and six were incorrectly classified as block concrete cracks. Similarly, of 27 images containing longitudinal concrete cracks, 21 were accurately classified as longitudinal and three were incorrectly classified as block concrete cracks. It is important to note that the accuracy of the classification algorithm was evaluated over a variety of concrete surfaces, without any prior training for the algorithm. This shows that the algorithm has the potential to be a viable component of a full-scale concrete crack detection system.

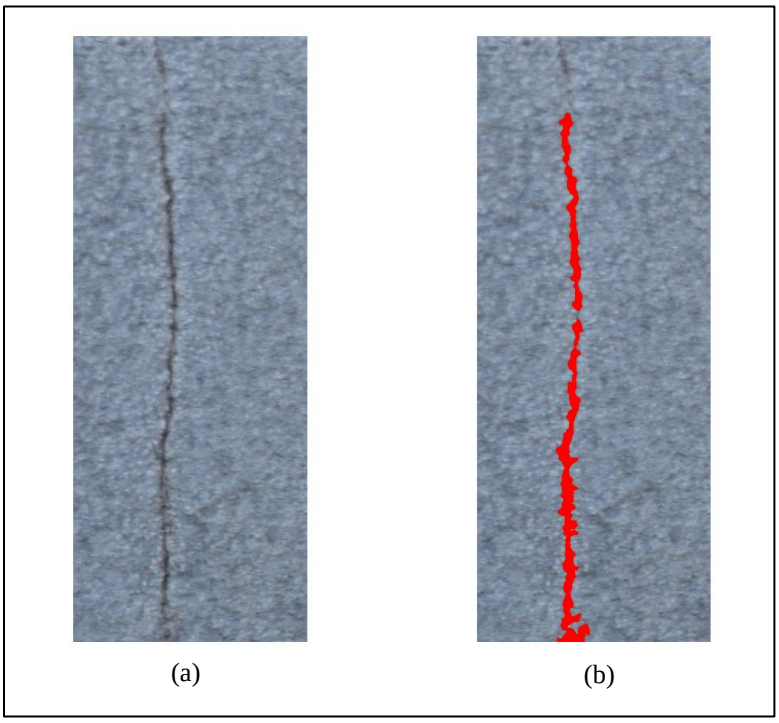

Figure 4-11 Example of (a) collected and (b) detected concrete crack images.

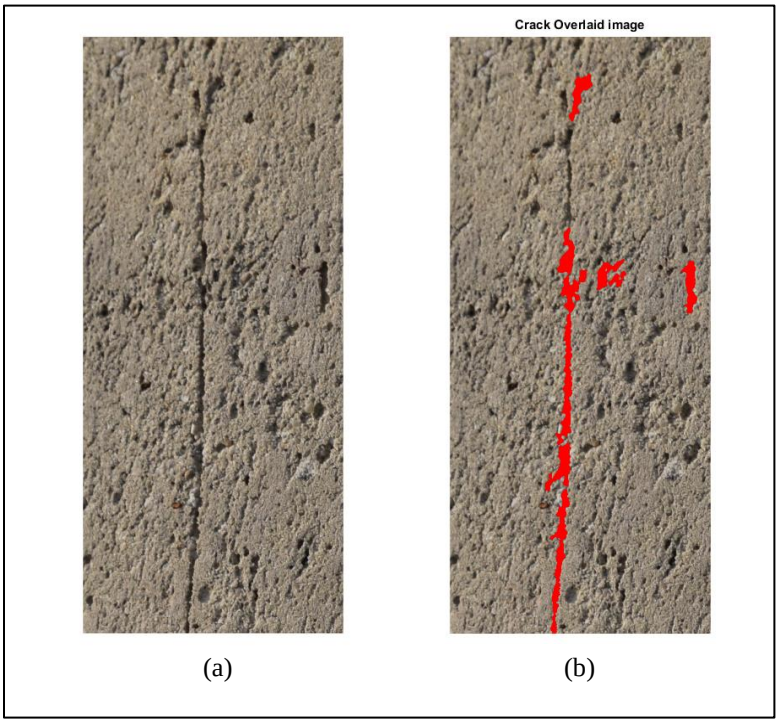

Figure 4-12 Example of more complex (a) collected and (b) detected concrete crack images,

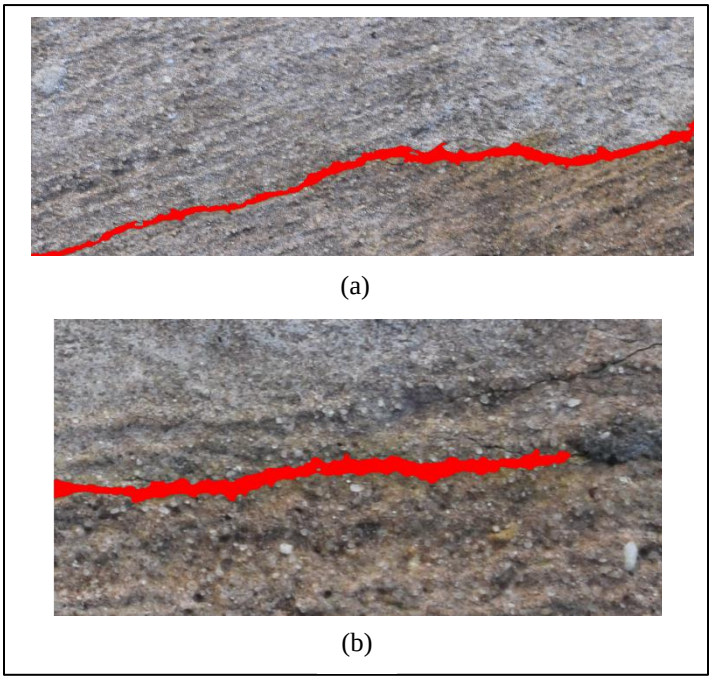

(a)

(b)

Figure 4-13 Examples of concrete crack detections on granular concrete.

Table 4-1 Confusion matrix for concrete crack classification using images collected with UAS

n = 53		**Predicted**		Total
		Transversal	Longitudinal	
Actual	Transversal	20	6	26
	Longitudinal	3	24	27
	Total:	23	30	
Accuracy	Transversal	20 / 26 =		77%
	Longitudinal	24 / 27 =		89%
	Overall	(20 + 24) / 53 =		83%

5 EVALUATION OF 3D MODELS FROM LIDAR DATA TO DETECT DISPLACEMENT OF BRIDGE COMPONENTS

This section describes the research approach taken to understand the applicability of 3D models developed from mobile LiDAR data to help identify signs of bridge settlement and displacement of bridge piles. The section also provides a description of the mobile LiDAR sensor used for data collections, approaches to align LiDAR data into a single coordinate system, and various tests conducted.

The approach employed to understand the applicability of 3D models from LiDAR data for bridge inspection purposes was twofold. First, LiDAR data were collected with the sensor attached to a tripod to control the position of the sensor during operation. Using this controlled method to conduct static data collection tests, questions regarding the applicability of 3D models for bridge inspection purposes could be addressed prior to incurring expenses associated with developing a UAS to hold the sensor, as well as costs associated with developing an approach to build 3D models without fully controlling the sensor's location. Assuming that the potential usability of the resulting 3D models was acceptable for bridge inspection purposes, the second step was to collect LiDAR data using a UAS, develop an effective approach to building 3D models from the data, and evaluate the expected usability of the models by comparing them to those developed during static tests.

5.1 MOBILE LIDAR SENSOR

The mobile LiDAR sensor used in this research project is a Velodyne HDL-32E (Figure 5-1a). In addition to being manufactured and tested to IP67 standards to meet rigorous environmental conditions, this sensor's size, weight, and resolution makes it a very good candidate for potential integration into a small UAS during Stage 2 of this project. The sensor features 32 laser/detector pairs physically aligned over a 41.34 degree vertical field of view (FOV) (ω) (+10.67 to -30.67) (Figure 5-1b). The sensor's lasers are classified as class 1 eye safe (i.e., incapable of producing damaging radiation levels). Its rotating head provides a 360 degree horizontal FOV (α) (Figure 5-1c). Furthermore, the sensor is capable of generating approximately 700,000 distance points per second and provides a measurement range of 70m (≈230 ft.) with a typical accuracy of ±2cm at a scan rate of 10 Hz.

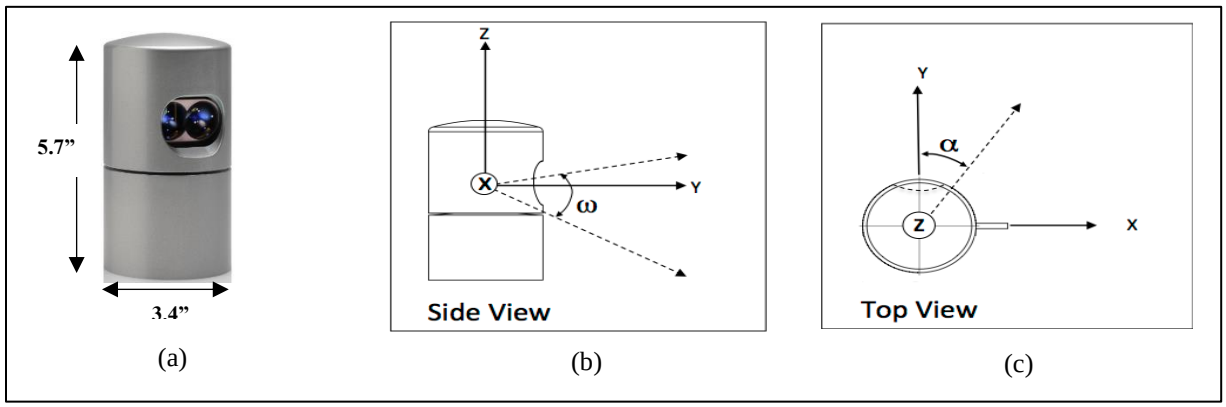

(a) (b) (c)

Figure 5-1 (a) Velodyne HDL-32E LiDAR sensor dimensions (b) side sensor view (c) top sensor view.

Data from the Velodyne mobile LiDAR sensor can be viewed using the manufacturer's visualization software called Veloview. However, after a thorough search for alternative software packages that provide additional 3D model viewing capabilities, the Quick Terrain Viewer software package was selected as the preferred option.

5.2 ALIGNMENT OF LIDAR DATA INTO COMMON COORDINATE SYSTEM

Fixed laser scanner LiDAR sensors are used to obtain 3D point clouds of target objects of interest. Point clouds represent distances from a target object to the sensor's origin. In other words, collected points for each individual LiDAR scan have coordinate values with respect to the sensor as the origin. In order to build a useful 3D model of a target of interest, multiple scans of the target must be collected at different locations and then aligned into a single 3D model. The objective of this alignment process is to bring all LiDAR points collected at different locations into a common coordinate reference frame. Aligning all scans into a common reference frame requires accurate knowledge of the LiDAR sensor with respect to some agreed-upon "global" coordinate system. The alignment of LiDAR data into a single coordinate system is called LiDAR data *registration*.

There are various approaches to aligning LiDAR data collected from different scans at different locations into a single coordinate system. One approach is to map each LiDAR point collected to global positioning system (GPS) standard parameters (i.e., latitude, longitude, and height). This mapping process of LiDAR points into GPS standard parameters (i.e., world coordinate system), considering any rotational sensor movements detected by an inertial measurement unit (IMU), is referred to as *geo-referencing*. A second approach is to work with a locally defined coordinate system by establishing a local position of the collection area as the origin. The idea is to precisely measure the location (i.e., one vertical and two horizontal displacements) of the LiDAR sensor with respect to this local origin. This information, coupled with sensor orientation data detected by an IMU, can be used to align individual scans into a single common reference frame by simply applying the appropriate horizontal and vertical displacements. A third approach also deals with using a locally defined coordinate system, but relies on algorithms instead of an IMU to solve for the rotation and translation of the LiDAR sensor used to collect the data. For example, the Iterative Closest Point (ICP) algorithm uses corresponding points (i.e., points from an original image that map to points from a rotated image) to calculate a sensor's rotation and translation that best aligns the points [*39*]. For the ICP algorithm to work properly, it is required that pairs of

LiDAR scans being processed by the algorithm are in close alignment to ensure that an object—or set of corresponding points—are found in both point sets.

5.3 Evaluating the Usability of 3D Models for Bridge Inspection Purposes using Controlled Sensor Locations

A small-scale mockup bridge was designed and constructed using polyvinyl chloride (PVC) material to serve as a testing platform to conduct controlled experiments prior to conducting more expensive field tests. The PVC bridge structure was designed to be modular and similar in shape to real-life railroad bridges (see Figure 5-2).

(a) (b)

Figure 5-2 (a) Real-life railroad bridge (b) PVC bridge structure for controlled experiments.

Initial tests involved controlling the location of the mobile LiDAR sensor during data collections by attaching it to a tripod. A customized tripod mount for the LiDAR sensor was constructed to improve its stability during data collections. The tripod mount helped to improve the quality of the data collected by fixing the sensor to specific locations, allowing more comprehensive analyses of retrieved point clouds during this stage of the research. A portable powering system for the mobile LiDAR sensor consisting of batteries, an alarm, and a voltage regulator was also developed during this stage.

The general solution approach for the controlled sensor location tests involved the following phases: test planning, data collection, alignment of LiDAR data into a common coordinate system, development of 3D models, and evaluating the use of the resulting models to identify structural deviations. The alignment/registration of LiDAR data to develop 3D models was completed using an approach based on the ICP algorithm, which is a locally defined coordinate system approach that does not require any GPS/IMU metadata (i.e., metadata-free approach to registration).

The modular bridge was assembled and leveled affix two mock abutments. Benchmark LiDAR scans were taken from four different positions around the bridge to get complete coverage of the structure. Following the benchmark scans, the research team proceeded to incline the structure at equal intervals–stacking 0.5 inch thick wooden stakes—to determine the capability to the LiDAR scans to help detect bridge movement (see Figure 5-3). More specifically, the team aimed to detect the AASHTO LRFD live load deflection limit of Span Length/800 for concrete vehicular bridges [*40*]. While current system specifications fall short of this value, the goal of this initial research task was to determine the level of deflections that could be identified; therefore, providing some knowledge regarding the current system's capabilities.

Figure 5-4 shows part of the testing setup. The experimental procedure included collecting LiDAR data at various controlled elevations (i.e., the height of the tripod could be manipulated) and distances from the bridge to develop dense point clouds. The LiDAR sensor fed the collected data to a workstation (not shown in the figure). Post analyses were then conducted in a laboratory setting to produce results such as those shown in Figure 5-5.

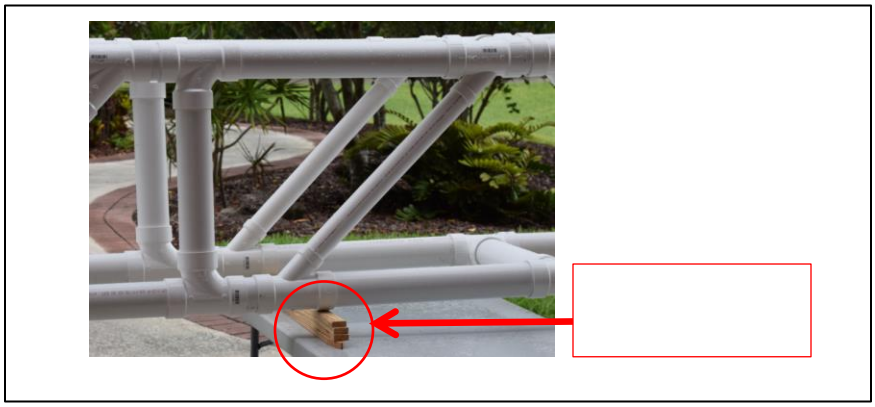

Figure 5-3 Wooden stakes of 0.5 inch thick for structure inclination.

Figure 5-4 Testing setup.

Data from the PVC bridge were collected at three different height inclinations and placing the LiDAR sensor at three different distances from the bridge (10, 20, and 30 feet). Table 5-1 shows the setting combinations that were used for data collection to develop nine 3D models. Each of the resulting 3D models were developed from only 20 LiDAR scans, where a single scan was associated with a known sensor location using the tripod. More specifically, the LiDAR sensor was raised 0.25 inch vertically for each scan. For each resulting 3D model, the height inclinations were measured using the Profile Analysis tool from the Quick Terrain Modeler software package. The results provided in Table 5-2 show detected versus actual bridge displacement heights. Due to the vertical FOV of the sensor's 32 lasers (Figure 5-1b), and given that the number of scans used for this experiment was not large, the density of the 3D models was expected to be affected by the distance of the sensor from the bridge during data collections. As expected, the 3D models obtained at a distance of 10 feet from the bridge were the densest, followed by the ones at 20 feet (see Figure 5-6). The 3D models at 30 feet were the blurriest (see Figure 5-6c). As shown in Table 5-2, error levels of measured versus true inclinations increased as the density of the 3D models decreased. These results demonstrate that even 3D models developed from a small number of LiDAR scans can potentially be used to effectively identify bridge deviations from a distance of up to 20 ft from a bridge.

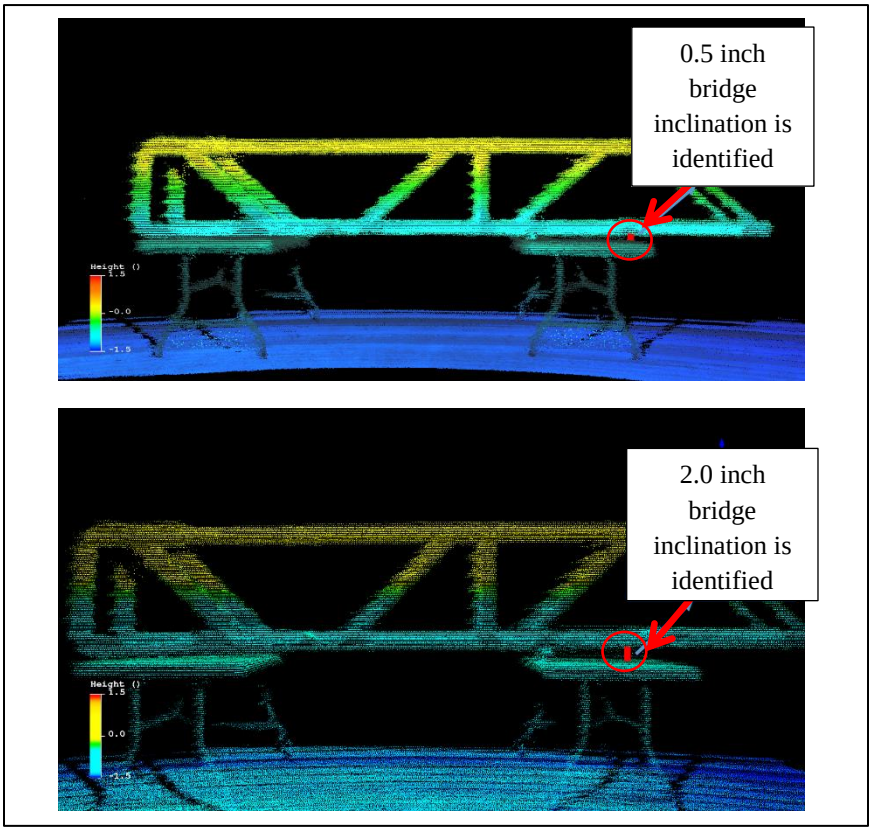

Figure 5-5 LiDAR 3D model showing 0.5 and 2.0 inch structural deviations (sensor was 10 feet from bridge).

Table 5-1 Settings for Outdoor Test

Distance (ft)	Bridge Inclination (in.)		
10	0.5	1	2
20	0.5	1	2
30	0.5	1	2

Table 5-2 Detected vs actual bridge displacements/inclinations

True Bridge Inclination (in.)	Distance of LiDAR Sensor from PVC Bridge (ft)	Measured Bridge Inclination using Software Tool (in.)	Error: Measured vs. True Inclination (in.)
0.5	10	0.40	-0.1
	20	0.40	-0.1
	30	0.00	-0.5
1.0	10	0.83	-0.17
	20	1.18	+0.18
	30	0.78	-0.22
2.0	10	1.96	-0.04
	20	2.36	+0.36
	30	2.75	+0.75

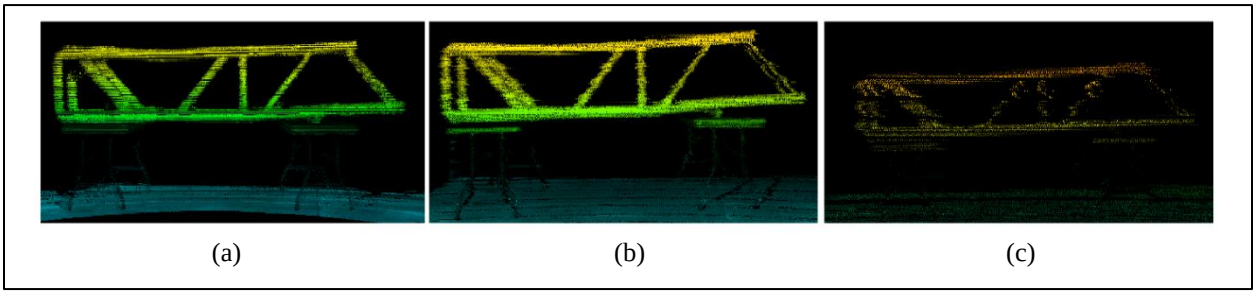

Figure 5-6 3D LiDAR models with 2 inch inclinations at (a) 10 ft, (b) 20 ft, and (c) 30 ft away from the structure.

5.4 Detecting Pile Deviations–Concrete Bridge in Melbourne, Florida

The research team conducted tests to gather mobile LiDAR data of a concrete bridge structure located in Melbourne, Florida. Some of the concrete piles that support this particular structure were angled or battered (see Figure 5-7a). These battered piles made this bridge an ideal field test candidate to evaluate whether 3D models developed from LiDAR data can be used to detect concrete pile deviations from a 90 degree angle. A local coordinate system was developed, and data from all the scans were manually registered to a user-defined reference scan—chosen arbitrarily from the data collected—using known translation/rotation values (sensor was affixed to a tripod mount). Matlab was used to reference the scans to the arbitrarily selected single scan, and the QuickTerrain Software was used to visualize them. In Figure 5-7b, a red triangle was manually drawn on the image to identify the column deviation from the 90 degree angle. This particular 3D model was developed from data collected with the LiDAR sensor located at a fixed horizontal distance from the bridge, and the density of the 3D model achieved by raising the sensor in the vertical direction for each scan.

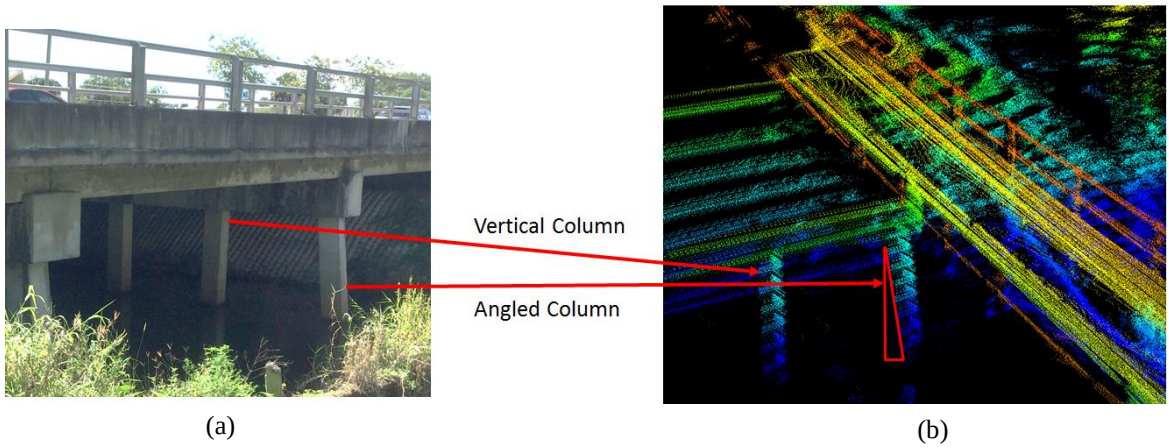

Figure 5-7 Mobile LiDAR 3D model showing vertical deviation of concrete battered pile.

5.5 Evaluation of 3D Models from LiDAR Data Collected with UAS

After demonstrating the potential value of 3D models for bridge inspection purposes using controlled sensor locations, the next step was to evaluate the applicability of 3D models developed from LiDAR data collected using a UAS instead. This section describes research efforts to develop a customized UAS with integrated LiDAR sensor and other subsystems for effective LiDAR data acquisition of bridge structures. The section also describes indoor and outdoor tests to develop 3D models of bridge structures and understand their potential to be used in practice during bridge inspections.

5.5.1 *CUSTOM-BUILT UAS FOR LIDAR DATA COLLECTION*

For this stage of the research project, a customized UAS was fully built by the research team to accommodate key subsystems such as the mobile LiDAR sensor and an onboard LiDAR data storage unit. The UAS, denoted multipurpose autonomous vehicle—flat eight (MAV-F8), was designed as a sensor testing platform capable of lifting relatively heavy and large sensor payloads. Figure 5-8a shows a snapshot of the fully integrated prototype MAV-F8 UAS, and Figure 5-8b shows a close up of the gimbal structure subsystem holding the LiDAR sensor and data storage subsystem. The objective of the data storage subsystem was to store LiDAR data during flight. This subsystem consisted of a Raspberry Pi 2 (RPi2) computer, SD card, 5GHz Wi-Fi dongle, and software code written to receive and process command messages via wireless links to start/stop data collections.

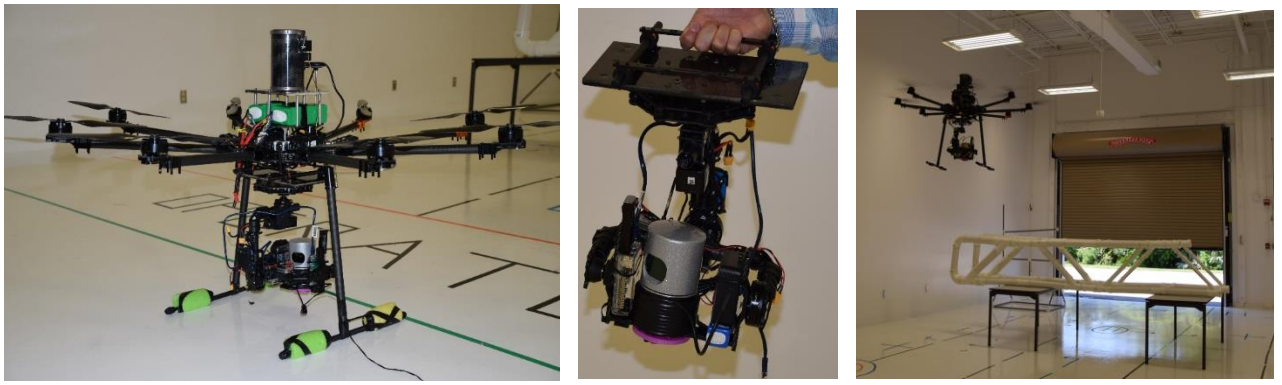

(a) (b) (c)

Figure 5-8 (a) Fully integrated UAS, (b) Gimbal structure, and (c) Indoor UAS flight around PVC bridge.

Systems engineering concepts were used to guide the development of the prototype MAV-F8 UAS. Safety parameters were considered throughout the design, development, and integration phases. Table 5-3 shows examples of various risk areas identified by the research team and some of the associated risk mitigation actions that took place during system integration.

Table 5-3 Examples of various key risk areas and associated risk mitigation actions

Risk Area	Risk Mitigation
Structural integrity	a. Used composite material b. Used precise development of aluminum parts via CNC process c. Used thread locks
Vibration reduction	a. Implemented isolation of parts b. Used dampeners to reduce vibrations c. Integrated a flight controller with vibration reduction capabilities d. Used well-balanced motors and propellers
Recovery system	a. Integrated an automatic parachute system b. Integrated floaters on arms and landing gear c. Implemented a one-motor failure compensation
Propulsion system	a. Integrated a dust proof propulsion system b. Integrated a water resistant propulsion system
Flight controller	Integrated a flight controller with the following characteristics: a. Dual GPS error and performance automated analysis b. Flight controller error and performance automated analysis c. Return home feature d. Takeoff and landing assist with automated landing gear folding e. Full autonomous mission programming f. Dual live telemetry downlinks

5.5.2 LiDAR Data Collection Tests with UAS

Indoor UAS flight tests were successfully conducted to collect LiDAR data of the same PVC bridge that was used for experimental tests during Stage 1 (see Figure 5-8c). Similar to the static tests described in Section 5.3, benchmark LiDAR scans were taken from various positions around the bridge to get a complete coverage of the structure. Afterwards, a side of the structure was inclined at 0.5 inch intervals to collect LiDAR data with the UAS, develop 3D models at each inclination level, and determine if collecting data with the UAS affected the usability of the resulting 3D models for bridge inspection purposes.

Figure 5-9 shows some of the resulting 3D models from data collected with the UAS. Visual examinations between 3D models developed from data collected with and without the UAS suggest that there is no noticeable difference between them. Therefore, based on the results from UAS indoor experiments, it is concluded that a UAS approach is highly capable of resulting in 3D models of high practical value during bridge inspections.

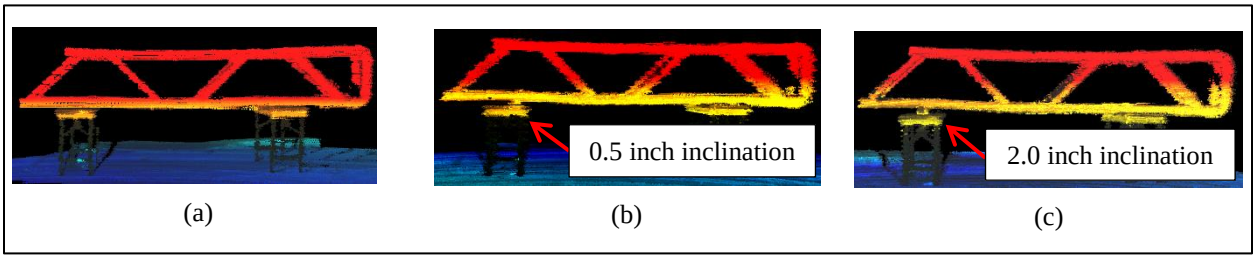

Figure 5-9 3D models from UAS-collected LiDAR data at (a) 0.0, (b) 0.5, and (c) 2.0 inch structural inclinations.

Outdoor UAS flight tests were also successfully conducted on a railroad bridge located in Palatka, Florida (see Figure 5-10). This bridge is owned by CSX Corporation, which is one of the leading transportation rail-based suppliers in the nation. The following list describes action items that took place to ensure a safe and productive flight mission:

- In full compliance with the latest FAA regulations, the UAS flights were conducted with FAA's approval—via the Section 333 process—and with a certified pilot operating the UAS.
- CSX personnel were present during the entire data collection exercises.
- The Florida Tech research team passed the CSX's Roadway Worker Training (RWT) program prior to the UAS flights.
- The Florida Tech research team complied with the use of required safety gear during the data collection exercises (i.e., steel toe boots, safety glasses, safety vest, and hard hat).
- CSX personnel and Florida Tech's PI met at the bridge site two weeks prior to the flights to go over flight plans and mission objectives.
- CSX obtained EC1 authority over the bridge during flights (i.e., no trains were to come through during UAS flights).
- CSX personnel briefed attendees on safety guidelines prior to the UAS flights.

Figure 5-11a shows an aerial image of the drawbridge portion of the railroad bridge, and Figure 5-11b shows its resulting 3D model from LiDAR data collected with the UAS. Similarly, Figure 5-12a shows an aerial image of a portion of the railroad track system, and Figure 5-12b shows its resulting 3D model from LiDAR data collected with the UAS.

Figure 5-10 CSX's railroad bridge in Palatka, Florida.

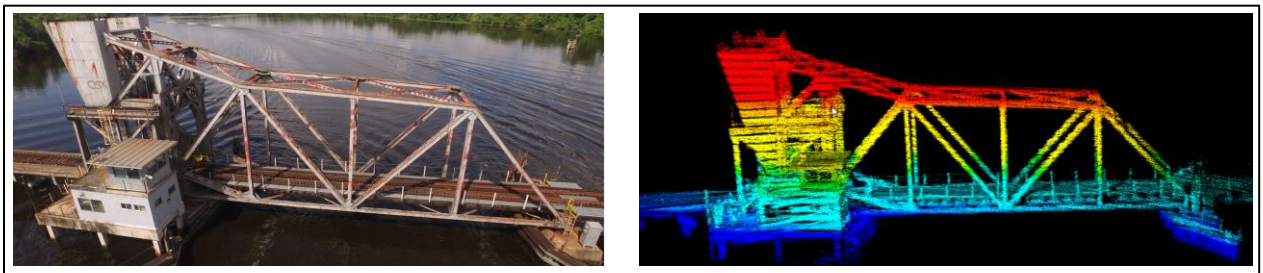

(a) (b)

Figure 5-11 (a) Image of railroad drawbridge (b) 3D model of drawbridge from LiDAR data.

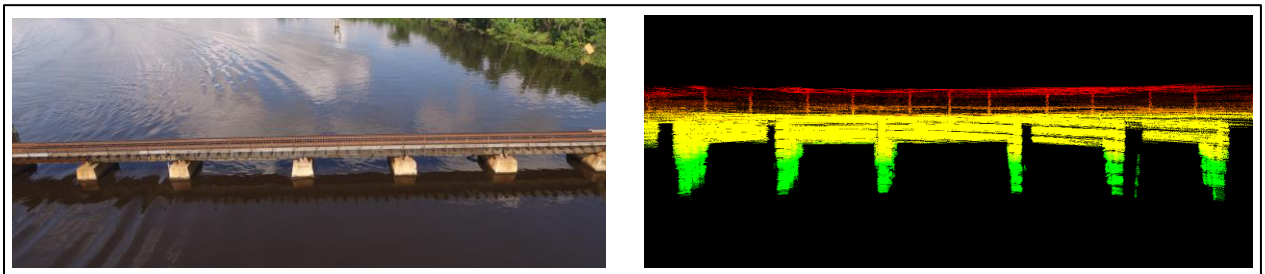

(a) (b)

Figure 5-12 (a) Image of railroad deck plate girder bridge system (b) Corresponding 3D model from LiDAR data.

6 CONCLUSIONS AND FUTURE RESEARCH

The overall objective of this research study was to investigate the applicability of two remote sensing approaches—based on LiDAR and imaging sensors—to help detect concrete cracks and displacement of bridge components. This overall objective was decomposed into three research objectives. The first research objective included developing and evaluating prototype image processing algorithms for concrete crack detection and classification. The second research objective

included developing and evaluating 3D models from LiDAR data to identify signs of bridge component displacements. The third research objective included evaluating the effects to the image processing algorithms and 3D models with data collected using a UAS. The solution approach to address these three research objectives was divided into two project stages. The first two research objectives corresponded to project stage 1, and the third research objective corresponded to project stage 2. Research questions corresponding to both project stages and their related research objectives were developed to guide the overall research study.

A literature review effort was conducted to gain insights from research studies that dealt with image processing techniques for concrete crack detection and classification, as well as studies that developed 3D models with LiDAR data for transportation infrastructure applications. Of particular importance was to identify possible gaps in previous studies that could have affected their implementation in practice (i.e., practical value). The following list provides a description of some key findings that resulted from the literature review effort:

- Most studies focus on the problem of detecting and classifying concrete cracks using as input images that only contain cracks (i.e., without any other background objects such as trees or other bridge components).
- There is no completely automatic system that performs crack detection and classification on images that contain both crack and non-crack objects (such as pipes, debris, trees, people). The problem of detecting cracks in the presence of these other objects is a significant problem that has not been addressed sufficiently.
- One of the main drawbacks of image processing methods proposed in the literature is that the detection results contain a significant number of false detections and false negatives if applied to images with different backgrounds (i.e., the performance of the method is highly dependent on the surface texture).
- The literature highlights the potential for using LiDAR for structural inspections due to the ability of data collection during day and night, minimization of personnel safety issues, minimization of data collection time, and potential reduction of costs.
- Some of the challenges for effective implementation of LiDAR technology include inspectors' lack of experience with remote sensing techniques, data management challenges due to enormous amounts of data, and software limitations.
- Studies that involve both UAVs and LiDAR systems for the specific purpose of bridge inspections are very scarce, and for inspection of railroad bridges are nonexistent. This lack of studies presents an opportunity to investigate the use of a LiDAR-UAV system for railroad bridge inspections.

Prototype image processing algorithms were developed to detect and classify concrete cracks. For the detection problem, a five-step algorithm was developed in Matlab. The algorithm was based on an unsupervised learning approach. The purpose of the algorithm was to extract pixels that belong to concrete cracks from images. For the classification problem, the objective was to process the resulting binary images from the detection algorithm to identify cracks as transversal, longitudinal, block, or alligator. The algorithms were tested with images collected from field tests. The images included different types of concrete cracks, along with various types of noise factors. The algorithms were successful in detecting and classifying different types of concrete cracks from various images. Contrary to previous studies found in the academic literature, these images were not "clean." That is, the images were collected from field tests and used as inputs to the detection algorithm without any preprocessing activity.

Various tests were conducted to address the research question regarding the applicability of 3D models developed from mobile LiDAR data to help identify signs of bridge settlement and displacement of bridge columns. The mobile LiDAR sensor used for data collection was a Velodyne HDL-32E. The first set of tests involved LiDAR data acquisition using a controlled sensor location approach. For these tests, a customized power supply system was developed to improve the sensor's mobility to various test locations. A customized tripod mount was also developed to control the sensor's position, thus facilitating the alignment of LiDAR data into a locally defined coordinate system to develop usable 3D models.

The general solution approach involved test planning, collecting data, aligning LiDAR data into a common coordinate system, developing 3D models, and evaluating the use of the resulting models to identify structural deviations. A mockup bridge structure was developed using PVC material to conduct initial experiments prior to conducting more expensive field tests. Prior to data collection, the LiDAR sensor was placed on the tripod mount at a distance of *x* feet from the PVC

structure, and a portion of the PVC structure was inclined *y* inches using 0.5 inches thick wooden stakes. The resulting 3D models showed that a 0.5 inch inclination was easily identified with the sensor located 10 feet from the structure, and using only 20 LiDAR scans. A field test was also successfully conducted to evaluate the applicability of 3D models from LiDAR data to help detect horizontal displacements of bridge components. It can be safely assumed that more scans at different sensor locations would result in denser 3D models, which would improve the usability of the 3D models for detecting vertical and horizontal displacement of bridge components. Overall, results highlighted the potential value of 3D models for bridge inspection purposes using controlled sensor locations,

The next step of the research effort was to evaluate the applicability of 3D models developed from LiDAR data collected using a UAS instead. To achieve this objective, a customized UAS with integrated LiDAR sensor and other subsystems was developed for effective LiDAR data acquisition of bridge structures. Indoor and outdoor UAS tests were conducted to collect LiDAR data of bridge structures for developing 3D models. Comparisons between the resulting 3D models from the UAS data acquisition approach versus those from the controlled sensor location approach indicated that there was no noticeable difference between them. It was concluded that a UAS approach is highly capable of resulting in 3D models of high practical value during bridge inspections.

Results from this initial research effort positively highlighted the potential practical value from using UAS and sensor technology for bridge inspection purposes. Industry support from CSX and FDOT throughout this research effort was essential to fully address the research questions that guided this study. The overall consensus from industry partners was that this technology has the potential to mature into a bridge inspection system that could positively and significantly impact performance, effectiveness, and safety associated with bridge inspections. Some future research directions that were identified to realize such a system include:

- Design and develop a small UAS to meet critical mission requirements specific to bridge inspections (e.g., maneuverability in tight spaces, extended flight durations, water proof capabilities, onboard computer for data storage and/or real-time data transmission)
- Automatic detection of concrete and steel cracks using a deep learning approach
- Automatic development of crack maps for bridge structures
- Software that will integrate data from various sensor types (e.g., LiDAR, infrared, imaging)
- Full integration of geo-location data to develop more detailed 3D models from LiDAR point clouds
- Software to automate the process of determining bridge orientation and measuring deviations of bridge components from 3D models developed from LiDAR data (this would include a visualization software)
- Add capability for autonomous (or semi-autonomous) UAS flights to collect sensor data of a bridge
- Conduct extensive outside field tests to fully evaluate the capability of UAS for bridge inspection purposes
- Develop studies to compare the costs/benefits from using current versus UAS approaches to bridge inspections
- Develop an implementation plan for DOTs and other entities to incorporate UAS as tools for bridge inspections

7 REFERENCES

[1] Casas, J. and P. Cruz, "Fiber optic sensors for bridge monitoring," *J. Bridg. Eng.*, 2003.

[2] Lee, B.Y., Y.Y. Kim, S.-T. Yi, and J.-K. Kim, "Automated image processing technique for detecting and analysing concrete surface cracks," *Struct. Infrastruct. Eng.*, pp. 1–11, Feb. 2011.

[3] Chambon, S. and J.M. Moliard, "Automatic road pavement assessment with image processing: Review and comparison," *Int. J. Geophys.*, 2011.

[4] Ahlborn, J., T.M. Shuchman, R. Sutter, L. Brooks, C. Harris, and D. Burns, "An Evaluation of Commercially Available Remote Sensors for Assessing Highway Bridge Condition," Ann Arbor, Mich., 2010.

[5] Yen, W.-H., G. Chen, I. Buckle, T. Allen, and D. Alzamora, *Post-Earthquake Reconnaissance Report on Transportation Infrastructure: Impact of the February 27, 2010, Offshore Maule Earthquake in Chile*, FHWA-HRT-11-030, Mar. 2011.

[6] Bray, J., B. Verma, X. Li, and W. He, "A Neural Network-based Technique for Automatic Classification of Road Cracks," in *International Joint Conference on Neural Networks*, pp. 907–912, 2006.

[7] Cheng, H.D. and M. Miyojim, "Novel System for Automatic Pavement Distress Detection," *J. Comput. Civ. Eng.*, Vol. 12, No. 3, pp. 145–152, 1998.

[8] Coster, M. and J.-L. Chermant, "Image analysis and mathematical morphology for civil engineering materials," *Cem. Concr. Compos.*, Vol. 23, No. 2–3, pp. 133–151, 2001.

[9] Huang, Y.and B. Xu, "Automatic inspection of pavement cracking distress," *J. Electron. Imaging*, Vol. 15, No. 1, p. 013017, 2006.

[10] Li, Q. and X. Liu, "Novel approach to pavement image segmentation based on neighboring difference histogram method," *Proc. - 1st Int. Congr. Image Signal Process, CISP 2008*, Vol. 2, pp. 792–796, 2008.

[11] Olivera, H. and P.L. Correia, "Automatic road crack detection and characterization," *IEEE Trans. Intell. Transp. Syst.*, Vol. 14, No. 1, pp. 155–168, 2013.

[12] Coudray, N., et al., "Multi-resolution approach for fine structure extraction: Application and validation on road images," *Computer* (*Long. Beach. Calif*)., pp. 17–21, May 2010.

[13] Chanda, S., G. Bu, H. Guan, J. Jo, U. Pal, Y. Loo, and M. Blumenstein, "Automatic Bridge Crack Detection—A Texture Analysis-Based Approach," in *Artifical Neural Networks in Pattern Recognition*, Springer International, pp. 193–203, 2014.

[14] Yamaguchi, T., S. Nakamura, R. Saegusa, and S. Hashimoto, "Image-based crack detection for real concrete surfaces," *IEEJ Trans. Electr. Electron. Eng.*, Vol. 3, No. 1, pp. 128–135, 2008.

[15] Wu, H., R. Zhao, and B. Li, "Crack image processing using probability based threshold," *2011 Int. Conf. Multimed. Technol.*, Vol. 2, pp. 3904–3907, 2011.

[16] Moon, H. and J. Kim, "Inteligent Crack Detecting Algorithm on Concrete Crack Images Using Neural Networks," in *Proceedings of the 28th ISARC, Seoul, Korea*, pp. 1461–1467, 2011.

[17] Yamaguchi, T., S. Nakamura, and S. Hashimoto, "An efficient crack detection method using percolation-based image processing," *2008 3rd IEEE Conf. Ind. Electron. Appl.*, pp. 1875–1880, 2008.

[18] Choudhray, G.K. and S. Dey, "Crack detection in concrete surfaces using image processing, fuzzy logic, and neural networks," *2012 IEEE Fifth Int. Conf. Adv. Comput. Intell.*, pp. 404–411, 2012.

[19] Tanaka, N. and K. Uematsu, "A Crack Detection Method in Road Surface Images Using Morphology," in *Workshop on Machine Vision Applications*, pp. 1–4, 1998.

[20] Elbehiery, H., A. Hefnawy, and M. Elewa, "Surface Defects Detection for Ceramic Tiles Using Image Processing and Morphological Techniques," *Proc. World Acad. Sci. Eng. Technol.* Vol. 5, No. 5, pp. 158–162, 2005.

[21] Oliveira, H. and P.L. Correia, "Identifying and retrieving distress images from road pavement surveys," *Proc. - Int. Conf. Image Process. ICIP*, pp. 57–60, 2008.

[22] Abdel-Qader, I., O. Abudayyeh, and M.E. Kelly, "Analysis of Edge-Detection Techniques for Crack

Identification in Bridges," *J. Comput. Civ. Eng.*, Vol. 17, No. 4, pp. 255–263, 2003.

[23] Zhou, J., "Wavelet-based pavement distress detection and evaluation," *Opt. Eng.*, Vol. 45, No. 2, p. 027007, 2006.

[24] Subirats, P. and J. Dumoulin, "Automation of pavement surface crack detection using the continuous wavelet transform," *Image Process. 2006 ...*, Vol. 1, No. 1, pp. 3037–3040, 2006.

[25] Ma, C.X., C.X. Zhao, and Y.K. Hou, "Pavement distress detection based on nonsubsampled contourlet transform," *Proc. - Int. Conf. Comput. Sci. Softw. Eng. CSSE 2008*, Vol. 1, pp. 28–31, 2008.

[26] Schmidt, B., "Automated Pavement Cracking Assessment Equipment: State of the Art," in *Routes Roads World Road Association*, 2003, pp. 35–44.

[27] Ecker, M. and R. Vincent, "Light Detection and Ranging (LiDAR) Technology Evaluation," Oct. 2010.

[28] Chang, J.C., D.J. Findley, M.K. Tsai, and C.M. Cunningham, "Infrastructure Investment Protection with LiDAR," 2012.

[29] Jaselskis, E.J., Z. Gao, A. Welch, and D. O'Brien, "Pilot Study on Laser Scanning Technology for Transportation Projects," 2003, Aug. 2003.

[30] Demann, A., "LiDAR/3D High Density Scanning (HDS) Bridge Scan/Model Project-Taggart Bridge," May 2010.

[31] Lasky, T.A., B. Ravani, and K.S. Yen, "LiDAR for Data Efficiency," Sept. 2011.

[32] Liu, W., S. Chen, and E. Hauser, "LiDAR-based bridge structure defect detection," *Exp. Tech.*, Vol. 35, No. 6, pp. 27–34, 2011.

[33] Yin, Z., C. Seto, and Y. Mao, "Develop a UAV Platform for Automated Bridge Inspection," 2015.

[34] Moller, P. (Aerorobotics), "CALTRANS Bridge Inspection Aerial Robot," 2008.

[35] Barfuss, S.L., A. Jensen, and S. Clemens, "Evaluation and Development of UAV for UDOT Needs," July 2012.

[36] Otero, L.D., *Proof of Concept for Using Unmanned Aerial Vehicles for High Mast Pole and Bridge Inspections*, FDOT Report No. BDV 28 977-02, 2015.

[37] Gonzalez, E., C. Rafael, and R. Woods, *Digital Image Processing*, 3rd ed., Prentice Hall, New Jersey. 2008.

[38] Perona, P. and J. Malik, "Scale-space and edge detection using anisotropic diffusion," *IEEE Trans. Pattern Anal. Mach. Intell.*, Vol. 12, No. 7, 1990.

[39] Besl, P.J. and N.D. McKay, "Method for registration of 3-D shapes," in *SPIE 1611, Sensor Fusion IV: Control Paradigms and Data Structures*, pp. 586–606, 1992.

[40] "American Association of State Highway and Transportation Officials (AASHTO)," 2014.